Transport Properties of Strongly Correlated Electrons in Quantum Dots Studied with a Simple Circuit Model

G. B. Martins,[1,*] C. A. Büsser,[2,3] K. A. Al-Hassanieh,[2,3,4] E. V. Anda,[5] A. Moreo,[2,3] and E. Dagotto[2,3]

[1]*Department of Physics, Oakland University, Rochester, Michigan 48309, USA*

[2]*Condensed Matter Sciences Division, Oak Ridge National Laboratory, Oak Ridge, Tennessee 37831, USA*

[3]*Department of Physics and Astronomy, The University of Tennessee, Knoxville, Tennessee 37996, USA*

[4]*National High Magnetic Field Laboratory and Department of Physics, Florida State University, Tallahassee, Florida 32306, USA*

[5]*Departamento de Física, Pontifícia Universidade Católica do Rio de Janeiro, 22453-900, Brazil*

(Received 29 April 2005; published 13 February 2006)

Numerical calculations are shown to reproduce the main results of recent experiments involving nonlocal spin control in quantum dots [Craig *et al.*, Science **304**, 565 (2004).]. In particular, the experimentally reported zero-bias-peak splitting is clearly observed in our studies. To understand these results, a simple ''circuit model'' is introduced and shown to qualitatively describe the experiments. The main idea is that the splitting originates in a Fano antiresonance, which is caused by having one quantum dot side connected in relation to the current's path. This scenario provides an explanation of the results of Craig *et al.* that is an alternative to the RKKY proposal, also addressed here.

DOI: 10.1103/PhysRevLett.96.066802 PACS numbers: 73.63.Kv, 71.27.+a, 73.23.Hk, 73.63.−b

The observation of the Kondo effect in a single quantum dot (QD) [1] and the subsequent theoretical and experimental studies of more complex structures, such as coupled QDs [2], has provided impetus for the analysis of more elaborate systems. In a recent seminal work, Craig *et al.* [3] report on the possible laboratory realization of the two-impurity Kondo system. Two similar QDs are coupled through an open conducting central region (CR). A finite bias is applied to one of the QDs (QD1 from now on) as well as to the CR, while the other QD (QD2) is kept at constant gate potential. The differential conductance of QD1 is then measured for different charge states of QD2 and different values of its coupling to the CR. The main result was the suppression and splitting of the zero-bias anomaly (ZBA) in QD1 by changing the occupancy of QD2 from an even to an odd number of electrons and by increasing its coupling to the CR. A Ruderman-Kittel-Kasuya-Yosida (RKKY) interaction between the QDs was suggested as an explanation for the observed effects [4,5]. The importance of the experiments of Craig *et al.* cannot be overstated: the possibility of performing nonlocal spin control in a system with two lateral QDs has potential applications in QD-based quantum computing [6].

In this Letter, numerical simulations in good agreement with the experiments are presented. The central conclusion of this work is that our computational data, and as a consequence the experimental results, can be explained using a very simple ''circuit model,'' where one of the elements is a T-connected QD that has an intrinsic reduction of conductance with varying biases. This proposal is an alternative to the more standard RKKY ideas. Figure 1(a) depicts the experimental setup used in the measurements of Craig *et al.* [3] with the labeling used in this Letter. Figure 1(b) is a schematic representation of the system, introducing two different tunneling parameters (hopping matrix elements t' and t'') and the Coulomb repulsion U in each QD (assumed the same for simplicity). To model this system, the Anderson impurity Hamiltonian is used for both QDs:

$$H_{\mathrm{d}} = \sum_{i=1,2;\sigma} [(U/2) n_{i\sigma} n_{i\bar{\sigma}} + V_{\mathrm{gi}} n_{i\sigma}], \tag{1}$$

where the first term represents the usual Coulomb repulsion between two electrons in the same QD, and the second term is the effect of the gate potential V_{gi} over each QD. QD1 is directly connected to the left lead and to the CR with hopping amplitude t', while QD2 is connected only to the CR (with hopping amplitude t''), which itself is connected to the right lead with hopping amplitude t (which is also the hopping amplitude in both leads, and our energy scale). In summary,

$$H_{\mathrm{leads}} = t \sum_{i\sigma} [c^{\dagger}_{li\sigma} c_{li+1\sigma} + c^{\dagger}_{ri\sigma} c_{ri+1\sigma} + \mathrm{H.c.}], \tag{2}$$

$$H_{12} = \sum_{\sigma} [t' c^{\dagger}_{1\sigma} (c_{l0\sigma} + c_{\mathrm{CR}\sigma}) + t'' c^{\dagger}_{2\sigma} c_{\mathrm{CR}\sigma} + t c^{\dagger}_{\mathrm{CR}\sigma} c_{r0\sigma} + \mathrm{H.c.}], \tag{3}$$

where $c^{\dagger}_{li\sigma}$ ($c^{\dagger}_{ri\sigma}$) creates an electron at site i with spin σ in the left (right) lead. The CR is composed of one tight-binding site [7], unless otherwise stated. Site ''0'' is the first site at the left (right) of QD1 (CR) in the left (right)

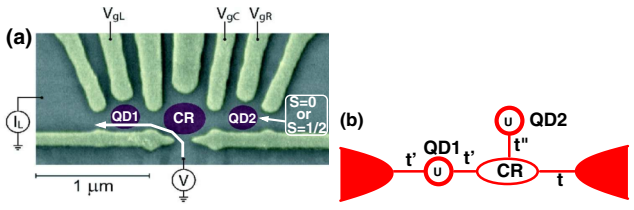

FIG. 1 (color online). (a) Experimental setup used in Ref. [3]. (b) Illustration of the model studied in this Letter (see text for details).

lead. The total Hamiltonian is $H_T = H_d + H_{leads} + H_{12}$. Note that for $V_{g1} = V_{g2} = -U/2$, the Hamiltonian is particle-hole symmetric. To calculate the conductance G, using the Keldysh formalism [8], a cluster containing the interacting dots and a few sites of the leads is solved exactly [9], the Green functions are calculated, and the leads are incorporated through a Dyson Equation embedding procedure [10]. All the results shown were obtained for $U = 0.5$, $t' = 0.2$, zero-bias, and zero temperature.

In Fig. 2, results for the conductance across QD1 (solid curves) and for the occupancy per spin orientation $\langle n_2 \rangle$ of QD2 (dashed curves) are presented. In Fig. 2(a), $t'' = 0.2$ and V_{g2} varies from -2.0 to -0.3. For $V_{g2} = -2.0$, QD2 is occupied by two electrons ($\langle n_2 \rangle = 1$) and the conductance of QD1 displays the characteristic Kondo behavior reported before [11]. For $V_{g2} = -0.35$ the average value of $\langle n_2 \rangle$ decreases to ≈ 0.7 (≈ 1.4 electrons in QD2) and $\langle n_2 \rangle$ now depends on V_{g1}. In addition, G decreases in comparison to the result obtained for $V_{g2} = -2.0$. Then, these numerical results are qualitatively in agreement with the experimental results shown in Fig. 2 of Craig *et al.* [3], namely, by decreasing the occupancy of QD2 from even to odd number of electrons, the ZBA in QD1 is suppressed. As V_{g2} is further increased (-0.3) a *qualitative* change

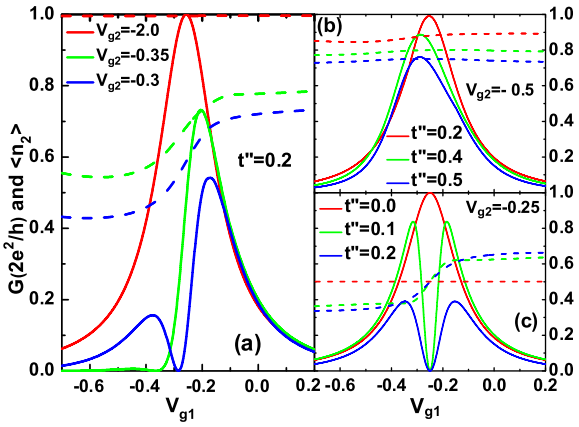

FIG. 2 (color online). (a) Variation of G with V_{g1} in QD1 (solid curves) and variation of $\langle n_2 \rangle$ [occupancy of QD2 per spin orientation (dashed curves)] for $t'' = 0.2$ and three different values of V_{g2}. For $V_{g2} = -2.0$ (red online), QD2 is occupied by 2 electrons ($\langle n_2 \rangle = 1$) for any V_{g1} and the conductance through QD1 is essentially the same as if QD2 were not present. For higher values of V_{g2}, the average value of $\langle n_2 \rangle$ decreases and becomes dependent on V_{g1} (decreasing for lower values of V_{g1}). This is accompanied by a suppression of the ZBA [for -0.35 (green online)] and also by a splitting of the ZBA [for $V_{g2} = -0.3$ (blue online)]. (b) Variation of G and $\langle n_2 \rangle$ with t'' (0.2, 0.4, 0.5) at a fixed value of $V_{g2} = -0.5$. As the value of t'' increases, the average value of $\langle n_2 \rangle$ decreases and this is again accompanied by a suppression of the ZBA. (c) Same as in (b), but now for $V_{g2} = -0.25$ (particle-hole symmetric point) and $t'' = 0.0$, 0.1, and 0.2. Note that G vanishes at $V_{g1} = -0.25$, where $\langle n_2 \rangle = 0.5$, for all finite values of t''. Note that $\langle n_1 \rangle \approx 0.5$ when $V_{g1} \approx -0.25$ for all curves.

occurs: For values of V_{g1} where $\langle n_2 \rangle \approx 0.5$ (QD2 singly occupied), the conductance of QD1 vanishes and therefore there is a narrow dip in G. This splitting of the ZBA is remarkably similar to that observed in Fig. 3(a) of Ref. [3], the experimental results. For finite-temperature calculations, the dip in G will not reach zero, resembling the experiments even better [12].

To further test the similarities between simulations and experiments, in Figs. 2(b) and 2(c) results for G and $\langle n_2 \rangle$ are shown for fixed V_{g2} and different t'' values. In Fig. 2(b), where $V_{g2} = -0.5$, as t'' increases from 0.2 to 0.5 there is only a slight decrease of G. This is accompanied by a slight decrease in the average value of $\langle n_2 \rangle$, from ≈ 0.9 to ≈ 0.7. A more dramatic change is obtained in Fig. 2(c), where $V_{g2} = -0.25$, and t'' varies from 0.0 to 0.2. By increasing t'' from 0.0 to 0.1, the ZBA is now split in two and $\langle n_2 \rangle$ acquires a dependence on V_{g1}. As t'' further increases (0.2), the two side peaks decrease and G still vanishes for $\langle n_2 \rangle = 0.5$ (one electron in QD2). Our calculations show that, if $\langle n_2 \rangle$ varies around 0.5, the dip in G is present for all finite values of t''. Comparing the results in Figs. 3(a) and 3(b) of Craig *et al.* in Ref. [3] with Figs. 2(c) and 2(b) in this Letter, respectively, one notices a striking similarity: The splitting of the ZBA observed in the experimental results [their Fig. 3(a)], when the number of electrons in the control QD is odd and the coupling to the CR is increased, is very similar to the dip in G for all finite-t'' curves in Fig. 2(c) (as mentioned above, at finite temperatures, one expects that the dip in G will not reach zero). When the occupancy of QD2 is even [Fig. 3(b) in the experimental results, Ref. [3], and Fig. 2(b) in this Letter], the G dependence on t'' is much less significant and the splitting of the ZBA does not occur [13].

What is the origin of these results? Below, it will be argued that a qualitative description of the results can be achieved by analyzing the two quantum dots through a so-called circuit model. This model starts with the conductance of each QD calculated separately, as independent elements of a circuit, and then the conductance of the ''complete circuit'' is obtained by combining the conductances of the two elements connected in series. Figure 3 describes schematically the steps involved in this approach. In Fig. 3(a), the complete system formed by QD1 and QD2 [shown in Fig. 1(b)] is divided into two components. QD1 is modeled as a QD connected directly to left (L) and right (R) leads, while QD2 is modeled as a side connected QD [14]. Figure 3(b) shows the respective conductances and occupancies for each independent element vs gate voltage, and Fig. 3(c) represents the scattering processes (represented by transmission and reflection amplitudes) that an electron undergoes while moving through the complete circuit. The superposition of all these processes leads to the total transmittance (proportional to the conductance) for the circuit model. This can be calculated in two ways: coherently or incoherently [15]. Since there is no qualitative difference between them, and in order to

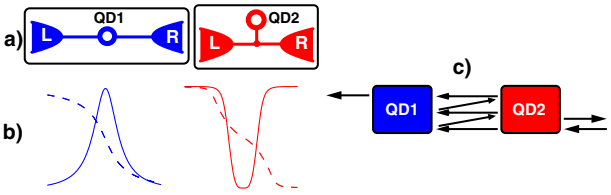

FIG. 3 (color online). Schematic representation of the main ideas behind the circuit model. In (a), the system represented in Fig. 1(b) is divided into its constituent elements: QD1 is modeled as a QD connected in series with the leads and QD2 is modeled as a side connected QD. The curves in (b) represent the conductance and occupancy of each separate circuit element vs the applied gate potential. (c) Schematic representation of how the two individual elements are connected to form the final "circuit:" Incident and reflected wave amplitudes are represented in the right side of QD2 by black arrows. A transmitted wave through QD2 undergoes multiple reflections between the two quantum dots until it is finally transmitted past QD1. The superposition of all these processes results in the final conductance for the circuit.

keep the simplicity of the model, we present the incoherent results. The equation which provides the final transmittance for the processes depicted in Fig. 3(c) is

$$T = \frac{T_1 T_2}{1 - R_1 R_2}, \tag{4}$$

where the transmittance $T_{1(2)}$ is proportional to the conductance for QD1(2), as depicted in Fig. 3(b), and $R_{1(2)} = 1 - T_{1(2)}$ are the reflectances. To calculate T, one needs to establish how T_2 depends on V_{g1}. The natural way to do that is to use the dependence of $\langle n_2 \rangle$ on V_{g1}, as depicted in Fig. 2, and then use the relation between conductance and occupancy, as shown in the right side of Fig. 3(b) (red curves online). In other words, the functional relation can be expressed as $T_2 = T_2(\langle n_2 \rangle(V_{g1}))$. It is not surprising that in a strongly correlated system like the one being analyzed here, the variation of the gate potential of QD1 will influence the charge occupancy of QD2, and in turn this will influence the conductance through QD1.

In Fig. 4, conductance results using Eq. (4) are shown for the same parameters as in Fig. 2. Although the quantitative agreement varies, there is good overall qualitative agreement. All the trends are correctly reproduced and some of the details are quite similar, such as, for example, the asymmetric shape of the curves at higher values of V_{g2} (-0.35 and -0.3) in Fig. 4(a). It is important to notice that there are *no* adjustable parameters in the circuit model here presented. The only input necessary is $\langle n_2 \rangle$ vs V_{g1}, which is obtained through a calculation for the complete system (values displayed for $\langle n_2 \rangle$ in Fig. 2). The success of the circuit model implies that the dip in G arises from the Fano antiresonance which cancels the conductance of QD2 [solid curve in the right panel of Fig. 3(b) (red online)]. The Fano antiresonance can be seen as a destructive interference process between two different trajectories an electron can take on its way to QD1: it can cross the CR

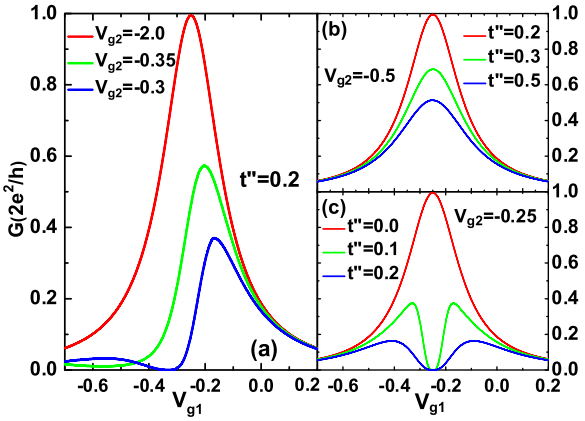

FIG. 4 (color online). Same as in Fig. 2, but now using the circuit model.

without passing through QD2; or it can visit QD2, return to the CR and then proceed to QD1 [14].

The similarities between the experimental results and our simulations suggest that our model and numerical technique have captured the essential physics of the experiments. However, these same experiments have also been explained using RKKY ideas [4,5]. Can our numerical results be also understood in this alternative context? To try to answer this question, several calculations were performed with different parameter values and number of sites in the CR [16]. In Fig. 5(a), results for spin correlations between QD1 and QD2 (denoted $\mathbf{S_1} \cdot \mathbf{S_2}$) are presented for the same parameters used in Fig. 2(c). At $t'' = 0.0$ QD1 and QD2 are uncorrelated as expected. As t'' increases to 0.1, and then 0.2, it is observed that in the region where G reaches its maximum value [see Fig. 2(c)], $\mathbf{S_1} \cdot \mathbf{S_2}$ also assumes a maximum value and it is positive [ferromagnetic (FM)]. For $t'' > 0.2$ (not shown), $\mathbf{S_1} \cdot \mathbf{S_2}$ saturates and starts decreasing. The maximum of $\mathbf{S_1} \cdot \mathbf{S_2}$, for all values of t'', decreases even further as the size of the CR increases [the results in Fig. 5(a) are for a CR with just one site]. In addition, the sign of $\mathbf{S_1} \cdot \mathbf{S_2}$ alternates as the size of the CR increases and the QDs move farther apart from each other. In Fig. 5(b), results for the spin correlation between QD1 and its neighboring site in the CR (denoted $\mathbf{S_1} \cdot \mathbf{S_c}$) is shown for the same parameters as in Fig. 5(a). $\mathbf{S_1} \cdot \mathbf{S_c}$ is a rough measure of the Kondo correlation in QD1, having a direct connection with the ZBA in Fig. 2(c). Indeed, for $t'' = 0.0$ when G reaches the unitary limit, a robust antiferromagnetic (AF) correlation develops between QD1 and its neighboring site in the CR. For $t'' = 0.1$, despite the narrow dip in G, the side peaks are still close to the unitary limit [see Fig. 2(c)] and $\mathbf{S_1} \cdot \mathbf{S_c}$ is still strongly AF. However, for $t'' = 0.2$, both G and $\mathbf{S_1} \cdot \mathbf{S_c}$ are strongly suppressed, in qualitative agreement with a suppressed ZBA due to a weakened Kondo resonance.

The results thus far seem to indicate that the CR could be mediating a long-range coupling between the QDs, with RKKY characteristics. However, the magnitude of the maximum value of $\mathbf{S_1} \cdot \mathbf{S_2}$ [see scale in Figs. 5(a) and

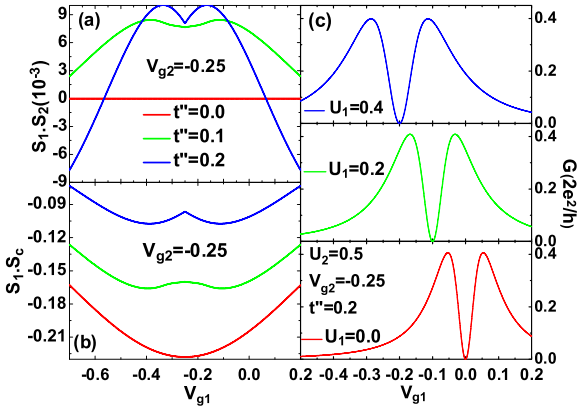

FIG. 5 (color online). (a) Spin correlation $\mathbf{S_1} \cdot \mathbf{S_2}$ between QD1 and QD2 for the same parameters as in Fig. 2(c). For $t'' = 0.0$ (red online), the two QDs are uncorrelated ($\mathbf{S_1} \cdot \mathbf{S_2} = 0$). For finite t'' [0.1 (green online) and 0.2 (blue online)], $\mathbf{S_1} \cdot \mathbf{S_2}$ is FM and reaches its maximum value in the region where G is maximum. (b) Kondo correlations $\mathbf{S_1} \cdot \mathbf{S_c}$ between QD1 and the central site for the same parameters as in (a). All values are AF and they decrease in amplitude as t'' increases, underscoring the decrease of the Kondo effect as the FM correlation between QD1 and QD2 increases [compare with (a)]. (c) Variation of G as U_1 (Hubbard interaction in QD1) assumes the values 0.4,0.2, and 0.0. Note that the dip in G becomes slightly narrower as U_1 decreases; however, it does not disappear.

5(b)] is too small to account for all the effects observed in the conductance in Fig. 2(c). One possible way of increasing $\mathbf{S_1} \cdot \mathbf{S_2}$ is by coupling QD1 more strongly to the CR than to the left lead. This was exactly the setup chosen in Ref. [3], where those authors performed the measurements with asymmetric couplings to the left (Γ_L) and right (Γ_{CR}) sides of QD1. In fact, the gate voltages in Fig. 1(a) were such that $\Gamma_{CR} \gg \Gamma_L$. In our model, this is equivalent to having an asymmetric t', with $t'_{CR} \gg t'_L$. An analysis of the results in this asymmetric regime indicates that the correlation between QD1 and QD2 does indeed increase. However, performing the calculations with the CR at a filling lower than one electron per site (half-filling), one observes that $\mathbf{S_1} \cdot \mathbf{S_2}$ is gradually suppressed as the electron filling falls to a more appropriate level to simulate the two-dimensional electron gas in the CR. Although one can argue that some of the dependence of the conductance of QD1 on the charge state of QD2 seen in Fig. 2 is associated with the correlations between the two dots, it is apparent that other effects are also present. This is dramatically exemplified by the fact that the cancellation of G in Fig. 2(c) occurs for *any* finite value of t'', and for $t'' \approx 0$ the two QDs will be virtually uncorrelated. The fact that the dip seen in the conductance in Fig. 2(c) is not dominantly caused by correlations between the dots can be made more clear by checking the results for the conductance as U_1 (Hubbard interaction in QD1) is reduced to zero. In Fig. 5(c), results for G are shown for 3 different values of U_1, for the same parameters as for $t'' = 0.2$ in Fig. 2(c). As U_1 decreases from 0.4 to 0.2, and then to 0.0, the dip in the conductance remains, only becoming narrower, indicating that its origin is not associated with many-body interactions, but more likely with cancellations typical of T geometries [14] that occur even in the noninteracting limit [17].

In summary, the numerical results qualitatively reproduce the main aspects of recent experiments [3] involving nonlocal spin control in nanostructures. The main result is that the splitting observed in the ZBA is caused by a cancellation in the conductance due to a destructive interference. This so-called Fano antiresonance has its origin in one of the dots being side connected to the current's path. A simple circuit model qualitatively reproduces the experiments and offers an alternative to a purely RKKY interpretation of the results, underscoring that a laboratory realization of the two-impurity Kondo system should avoid geometries susceptible to a Fano antiresonance.

C. B., K. A., A. M., and E. D. are supported by NSF Grant No. DMR 0454504, and G. M. by an OU internal grant.

*Corresponding author.
Email address: martins@oakland.edu

[1] D. Goldhaber-Gordon *et al.*, Nature (London) **391**, 156 (1998).
[2] W. G. van der Wiel *et al.*, Rev. Mod. Phys. **75**, 1 (2003).
[3] N. J. Craig *et al.*, Science **304**, 565 (2004).
[4] P. Simon *et al.*, Phys. Rev. Lett. **94**, 086602 (2005).
[5] M. G. Vavilov *et al.*, Phys. Rev. Lett. **94**, 086805 (2005).
[6] D. Loss *et al.*, Phys. Rev. A **57**, 120 (1998).
[7] Same results are obtained for a larger CR.
[8] Y. Meir *et al.*, Phys. Rev. Lett. **66**, 3048 (1991).
[9] Results shown have one site on each side. No significative size effects were observed with more sites.
[10] See V. Ferrari *et al.*, Phys. Rev. Lett. **82**, 5088 (1999).
[11] Removing QD2 results in essentially the same conductance as the one for $V_{g2} = -2.0$.
[12] R. Franco *et al.*, Phys. Rev. B **67**, 155301 (2003).
[13] Magnetic field dependence of the conductance was also calculated and the results agree with the description provided by Craig *et al.* (Ref. [3]) and with recent experiments involving Cobalt ions interacting with a gold nanocluster QD [H. B. Heersche *et al.*, Phys. Rev. Lett. **96**, 017205 (2006); see their Fig. 4(b)]: low field values restore a Kondo-like conductance, while higher fields produce again a splitting. In addition, conductance calculations for QD1 in a Coulomb blockade regime (sweeping V_{g2} instead of V_{g1}) will also be reported elsewhere.
[14] M. Sato *et al.*, Phys. Rev. Lett. **95**, 066801 (2005).
[15] S. Datta, *Electronic Transport in Mesoscopic Systems* (Cambridge University Press, Cambridge, England, 1995).
[16] A full discussion of results will be presented elsewhere.
[17] Figure 2b of Ref. [4] clearly implies that the ZBA splitting considerably increases with the strength of the RKKY interaction. In this respect, our Fig. 2(c) provides a better description of Fig. 3a of Ref. [3].